ELectronics EXpress

LETTER

IEICE Electronics Express, Vol.13, No.18, 1–8

A novel planar tri-band bandpass filter using stub-loaded resonators

Weiping Li[1,2a)], **Zongxi Tang**[1], **Haodong Lin**[1], **and Xin Cao**[1]

[1] *School of Electronic Engineering, University of Electronic Science and Technology of China, No.2006, Xiyuan Ave, West Hi-Tech Zone, Chengdu, 611731, China*

[2] *School of Information Engineering, East China Jiaotong University, No.88, Shuanggang Road, Nanchang, 330013, China*

a) *lwp8277@126.com*

Abstract: This letter presents a novel planar tri-band bandpass filter (BPF) using a set of stepped-impedance resonators (SIRs) and a short-circuited stub-loaded uniform impedance resonator. The former is designed to operate at the first and third passbands and the latter at the second passband. Corresponding equivalent circuit is analyzed by using the even-odd mode theory. Skirt selectivity is obtained due to source-load coupling. For validation, a tri-band BPF with compact size is designed, fabricated, and measured, its center frequencies are located at 2.4, 3.5, 5.15 GHz. Measured results show good performance on insertion loss and return loss.

Keywords: bandpass filter, even-odd mode theory, stub-loaded resonator, tri-band

Classification: Microwave and millimeter-wave devices, circuits, and modules

References

[1] W. Y. Chen, *et al.*: "Simple method to design a tri-band bandpass filter using asymmetric SIRs for GSM, Wimax and WLAN applications," Microw. Opt. Technol. Lett. **53** (2011) 1573 (DOI: 10.1002/mop.26037).

[2] B.-J. Chen, *et al.*: "Design of tri-band filters with improved band allocation," IEEE Trans. Microw. Theory Techn. **57** (2009) 1790 (DOI: 10.1109/TMTT.2009.2022888).

[3] W. Y. Chen, *et al.*: "A new tri-band bandpass filter based on stub-loaded step-impedance resonator," IEEE Microw. Wireless Compon. Lett. **22** (2012) 179 (DOI: 10.1109/LMWC.2012.2187884).

[4] F. C. Chen and Q. X. Chu: "Design of compact tri-band bandpass filters using assembled resonators," IEEE Trans. Microw. Theory Tech. **57** (2009) 165 (DOI: 10.1109/TMTT.2008.2008963).

[5] C. I. G. Hsu, *et al.*: "Tri-band bandpass filter with sharp passband skirts designed using tri-section SIRs," IEEE Microw. Wireless Compon. Lett. **18** (2008) 19 (DOI: 10.1109/LMWC.2007.911976).

[6] X. Lai, *et al.*: "Design of tri-band filter based on stub loaded resonator and DGS resonator," IEEE Microw. Wireless Compon. Lett. **20** (2010) 265 (DOI: 10.1109/LMWC.2010.2045584).

[7] J.-Z. Chen, *et al.*: "Fourth-order tri-band bandpass filter using square ring

© IEICE 2016

DOI: 10.1587/elex.13.20160605
Received June 20, 2016
Accepted June 27, 2016
Publicized July 11, 2016
Copyedited September 25, 2016

loaded resonators," Electron. Lett. **47** (2011) 858 (DOI: 10.1049/el.2010.3724).
[8] X. Y. Zhang, *et al.*: "Dual-band bandpass filter design using a novel feed scheme," IEEE Microw. Wireless Compon. Lett. **19** (2009) 350 (DOI: 10.1109/LMWC.2009.2020009).
[9] J.-S. Hong and M. J. Lancaster: *Microstrip Filters for RF/Microwave Applications* (Wiley, New York, 2001) 258.
[10] S. Sun and L. Zhu: "Wideband microstrip ring resonator bandpass filters under multiple resonances," IEEE Trans. Microw. Theory Techn. **55** (2007) 2176 (DOI: 10.1109/TMTT.2007.906510).
[11] H. W. Liu, *et al.*: "Tri-band microstrip bandpass filter using dual-mode stepped-impedance resonator," ETRI J. **35** (2013) 344 (DOI: 10.4218/etrij.13.0212.0319).
[12] X. Y. Zhang, *et al.*: "Dual-band bandpass filters using stub-loaded resonators," IEEE Microw. Wireless Compon. Lett. **17** (2007) 583 (DOI: 10.1109/LMWC.2007.901768).
[13] J.-S. Hong and M. J. Lancaster: *Microstrip Filters for RF/Microwave Applications* (Wiley, New York, 2001) 13.

1 Introduction

Tri-band bandpass filters (BPFs) are important building blocks in multi-band multi-standard wireless communication systems, such as global system for mobile communications (GSM), worldwide interoperability for microwave access (WiMAX) and wireless local area network (WLAN). In recent years, research on tri-band bandpass filters has become very popular and various design approaches have been proposed. In [1], a pair of asymmetric stepped-impedance resonators (SIRs) with parallel coupling arrangement was proposed to realize the tri-band responses. However, the selectivity of the passbands needs to be improved. As proposed in [2, 3], the traditional tri-band filters were popularly achieved by cascaded SIRs, which led to a large circuit size. Thus, a pair of tri-section SIRs using parallel coupling arrangement was adopted in order to reduce the size [4, 5]. Because of the dependence on the resonant frequencies, the tri-section SIRs suffered from the design complexity, especially in the analysis of resonant frequencies. Recently, tri-band BPFs also could be constructed using a stub-loaded resonator (SLR) with defected ground structure (DGS) resonator [6] and square ring loaded resonator [7]. Nevertheless, the passband selectivity still needs to be improved with the help of several transmission zeros. Therefore, more flexible design in the choice of band allocation and high selectivity is needed.

In this letter, a novel planar tri-band BPF for wireless communication applications is presented. The filter is constructed by a set of T-stub loaded SIRs and a short-circuited stub-loaded uniform impedance resonator, the former resonates at the first and third passbands and the latter at the second passband. Source-load coupling is introduced to produce extra transmission zeros which are close to passband edges, resulting in skirt selectivity and excellent band-to-band isolation. A tri-band BPF with three central frequencies at 3.50 GHz for WIMAX and 2.4, 5.15 GHz for WLAN is designed, fabricated and measured.

© IEICE 2016
DOI: 10.1587/elex.13.20160605
Received June 20, 2016
Accepted June 27, 2016
Publicized July 11, 2016
Copyedited September 25, 2016

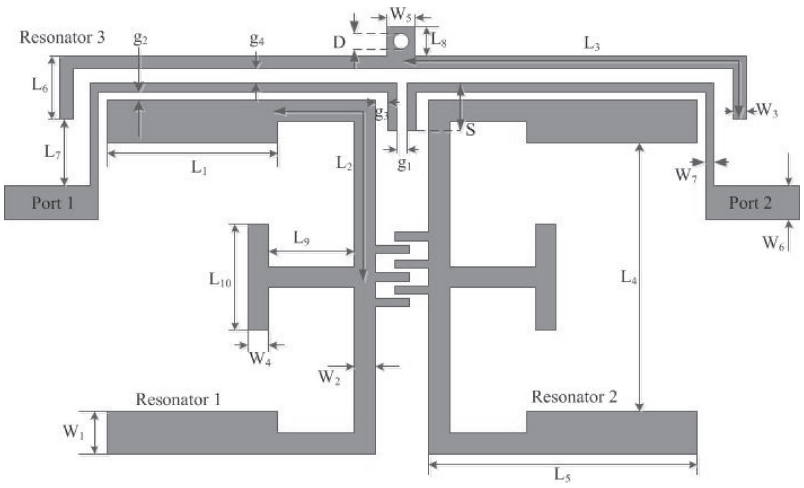

Fig. 1. Filter configuration

2 Design and analysis of the tri-band BPF

The configuration of the proposed tri-band BPF is depicted in Fig. 1. Resonator 1 and resonator 2 denoted by lengths (L_1, L_2) and widths (W_1, W_2) are SIRs operating at the first and third passband frequencies, i.e., f_1 and f_3. T-stub is located at the center plane of the SIR, thus, two modes can be excited. Since the structure of the SIR is symmetrical, the even- and odd-mode theory is applied to analyze its equivalent circuit, as shown in Fig. 2(a) and (b). An interdigital capacitor (IDC), as shown in Fig. 2(c) with its equivalent circuit [8], is utilized to realize inter-stage coupling, the finger length and width are denoted by L_C and W_C, respectively, the gap between the adjacent fingers is denoted by g_C. These parameters can be properly tuned to satisfy the coupling demand between resonator 1 and resonator 2 [9]. Here, θ_1, θ_2, θ_3 and θ_4 are electrical lengths of the sections of the lengths L_1, L_2, L_9, $L_{10}/2$, respectively, and Y_1, Y_2, Y_3, Y_4 are the characteristic admittances of the sections mentioned above. Y_3 and Y_4 are set equal to Y_2 for simplicity. Ignoring the input influences of the step discontinuity, the input admittance $Y_{in\text{-}even}$ and $Y_{in\text{-}odd}$ of the even- and odd mode SIR can be expressed as

$$Y_{in\text{-}even} = -jY_1 \frac{Y_2 + Y_1 \cot(\theta_2 + \theta_3 + \theta_4) \tan\theta_1}{Y_1 \cot(\theta_2 + \theta_3 + \theta_4) + Y_2 \tan\theta_1} \tag{1}$$

$$Y_{in\text{-}odd} = -jY_1 \frac{Y_2 - Y_1 \tan\theta_1 \tan\theta_2}{Y_1 \tan\theta_2 + Y_2 \tan\theta_1} \tag{2}$$

From the resonant condition $Y_{in\text{-}even} = 0$ and $Y_{in\text{-}odd} = 0$ [10], the resonant frequencies can be expressed as

$$R_Y + \cot(\theta_2 + \theta_3 + \theta_4) \tan\theta_1 = 0 (at\ f = f_{even}) \tag{3}$$

$$R_Y - \tan\theta_1 \tan\theta_2 = 0 (at\ f = f_{odd}) \tag{4}$$

where f_{even} and f_{odd} are the even- and odd-mode resonant frequencies of the proposed SIR, respectively. $R_Y = Y_2/Y_1$ is the admittance ratio.

From (3), the resonant frequencies of even-mode are decided by θ_1, θ_2, θ_3, θ_4 and R_Y. Also from (4), the resonant frequencies of odd-mode are decided by θ_1, θ_2 and R_Y. Thus, by tuning these parameters, f_{even} and f_{odd} can be properly placed in

© IEICE 2016
DOI: 10.1587/elex.13.20160605
Received June 20, 2016
Accepted June 27, 2016
Publicized July 11, 2016
Copyedited September 25, 2016

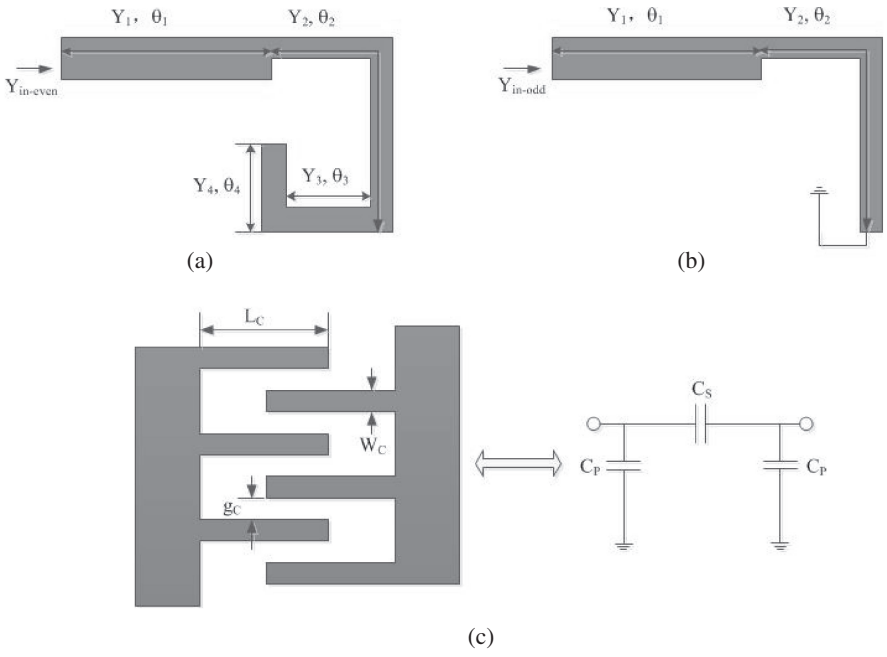

Fig. 2. (a) Even-mode equivalent circuit, (b) Odd-mode equivalent circuit, (c) Interdigital capacitor and its equivalent circuit

the desired passbands. From Fig. 2, the fundamental even- and odd-mode frequencies, f_{even1} and f_{odd1}, can be approximately estimated as

$$f_{even1} = \frac{c}{2\left(L_1 + L_2 + L_9 + \frac{L_{10}}{2}\right)\sqrt{\varepsilon_{eff}}} \tag{5}$$

$$f_{odd1} = \frac{c}{4(L_1 + L_2)\sqrt{\varepsilon_{eff}}} \tag{6}$$

where c is the speed of light in free space, $\overline{\varepsilon_{eff}} = \frac{\varepsilon_r + 1}{2} + \frac{\varepsilon_r - 1}{2}\left[\left(1 + 12\frac{h}{\bar{w}}\right)^{-\frac{1}{2}} + 0.04\left(1 - \frac{\bar{w}}{h}\right)^2\right]$, ε_r and h denote the relative dielectric constant and thickness of the substrate, respectively. $\bar{w}$ is equal to $(W_1 + W_2)/2$ [11].

It can be observed from (5) and (6) that under normal circumstance $\left(L_9 + \frac{L_{10}}{2} < 2(L_1 + L_2)\right)$, f_{even1} is higher than f_{odd1}, therefore, f_{odd1} is set to operate at the first passband, then f_{even1} can be moved to the higher frequency passband by tuning R_Y. The T-stub is loaded at the symmetric plane of SIR where the voltage is zero at f_{odd1}, adding the stub will not affect f_{odd1} [12]. Hence, the dimensions of the stub, expressed by L_9 and L_{10}, can be adjusted to control f_{even1} without altering f_{odd1}. Thus, f_{even1} can be adjusted to f_3 by simultaneously tuning R_Y, L_9 and L_{10}, which increases the design flexibility. Fig. 3 depicts the effect of the T-stub on the dual-mode characteristics. It can be seen that by tuning the length L_9 of the stub, f_{even1} is shifted effectively while there is almost no influence on f_{odd1}. The influence of L_{10} on f_{even1} is similar to that of L_9, the total length of the even-mode equivalent circuit becomes longer when the value of L_{10} (or L_9) is increased, which makes f_{even1} decrease.

© IEICE 2016
DOI: 10.1587/elex.13.20160605
Received June 20, 2016
Accepted June 27, 2016
Publicized July 11, 2016
Copyedited September 25, 2016

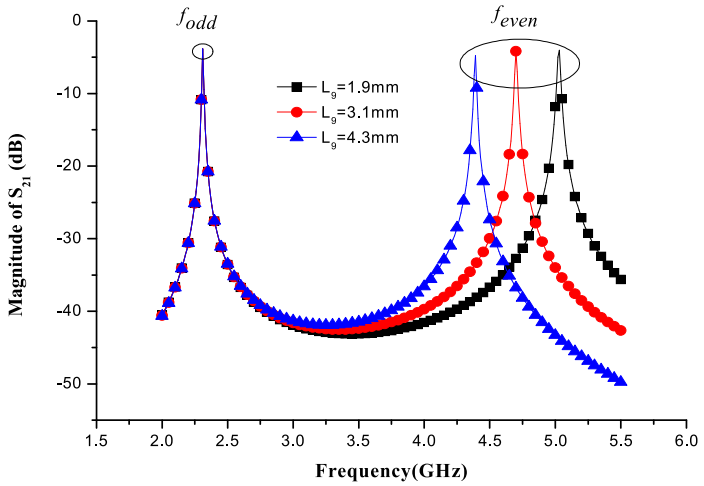

Fig. 3. Even-mode (f_{even}) and odd-mode (f_{odd}) frequencies with varied L_9

In Fig. 2(c), the equivalent circuit of IDC is an admittance π-network consists of C_p and C_s. The ABCD matrix of the π-network can be expressed as [13]:

$$\begin{Bmatrix} 1+\dfrac{C_p}{C_s} & -j\dfrac{1}{\omega C_s} \\ 2j\omega\left(C_p+\dfrac{{C_p}^2}{C_s}\right) & 1+\dfrac{C_p}{C_s} \end{Bmatrix} \tag{7}$$

where ω is operation frequency. The ABCD matrix of IDC can be obtained using full-wave simulation, by comparing the simulation results with (7), the values of C_p and C_s can be extracted at corresponding frequencies.

Resonator 3 is a short-circuited stub-loaded uniform impedance resonator, which is used to generate the passband at f_2. A pair of even- and odd-mode resonant frequencies can be excited and tuned by varying the length L_8 of the short-circuited stub. Two resonant frequencies at the second passband can be obtained by

$$f_{even2} = \frac{c}{4(L_3+L_8)\sqrt{\varepsilon_{eff}}} \tag{8}$$

$$f_{odd2} = \frac{c}{4L_3\sqrt{\varepsilon_{eff}}} \tag{9}$$

Considering the loading effect of resonators 1 and 2, the total length of resonator 3 is chosen slightly shorter than half guided wavelength at f_2.

The feedlines tapped by 50 Ω I/O ports are placed between the resonators, the required external quality factors at the passbands can be satisfied by properly adjusting the position of the feedlines. Also, source-load coupling can be implemented because of the coupling between the open ends of the feedlines, extra transmission zeros close to passband edges are generated, thus, sharper attenuation shirts of the passbands can be achieved.

3 Experimental results

For demonstration purpose, a tri-band BPF is implemented operating at 2.4 GHz, 3.5 GHz, and 5.15 GHz for WiMAX, and WLAN applications. The experimental

© IEICE 2016
DOI: 10.1587/elex.13.20160605
Received June 20, 2016
Accepted June 27, 2016
Publicized July 11, 2016
Copyedited September 25, 2016

filter is fabricated using the substrate Rogers 4350B with relative dielectric constant of 3.48, thickness of 0.508 mm and loss tangent $\delta = 0.0018$. Following the aforementioned design method, the dimension parameters of the tri-band filter are determined as tabulated in Table I. In addition, the finger number of the interdigital capacitor is 6 and the diameter of the viahole (represented by "D") is equal to 0.5 mm. The fundamental odd- and even-mode resonant frequencies of resonator 1 and resonator 2 are located at the desired first (2.4 GHz) and third (5.15 GHz) passbands respectively. Resonator 3 is designed to operate at the second (3.5 GHz) passband. The photograph of the fabricated filter is shown in Fig. 4.

Table I. Dimension parameters of the filter (unit: mm)

L_1	L_2	L_3	L_4	L_5	L_6	L_7	L_8
7.15	6.95	12.95	6.2	9.5	2.1	1.4	0.9
L_9	L_{10}	W_1	W_2	W_3	W_4	W_5	W_6
1.95	2.9	2.05	0.55	0.4	0.6	0.8	1.15
W_7	g_1	g_2	g_3	g_4	g_c	L_c	W_c
0.2	0.4	0.15	0.25	0.5	0.2	0.75	0.15

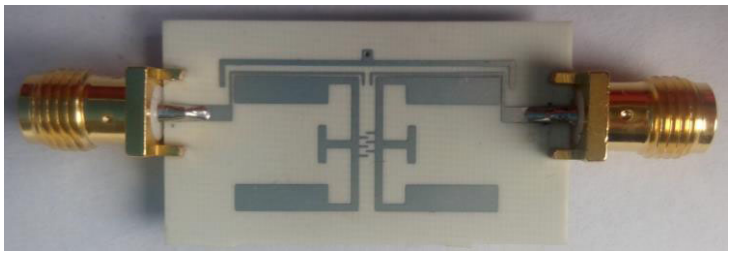

Fig. 4. Photograph of the fabricated tri-band BPF

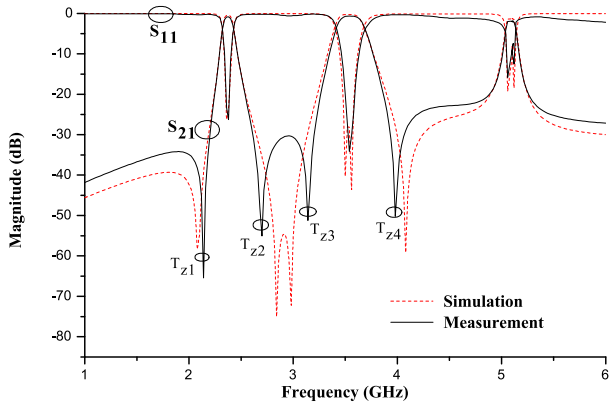

Fig. 5. Simulated and measured results of the proposed tri-band BPF

The simulation and measurement are accomplished by using Sonnet and Rohde & Schwarz's ZVA40 vector network analyzer. In Fig. 5, the simulated and measured results are illustrated. The measured passbands have insertion loss of 0.89 dB, 0.74 dB and 1.7 dB, return loss of 25.6 dB, 34.2 dB and 16 dB corresponding to 2.4, 3.5 and 5.15 GHz, respectively. Four transmission zeros (T_{zs}) are

© IEICE 2016
DOI: 10.1587/elex.13.20160605
Received June 20, 2016
Accepted June 27, 2016
Publicized July 11, 2016
Copyedited September 25, 2016

realized at 2.14, 2.7, 3.14 and 3.98 GHz. From the full-wave simulation results depicted in Fig. 6, it is observed that all the transmission zeros are generated by source-load coupling.

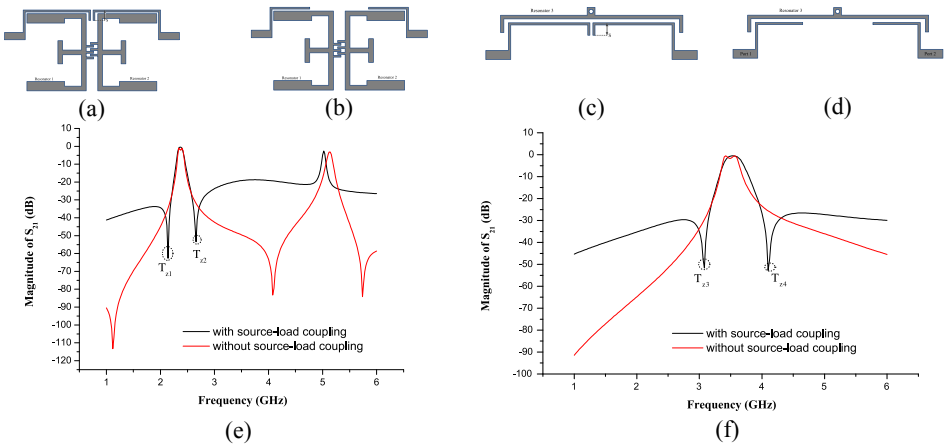

Fig. 6. (a) Resonator 1 and resonator 2 are fed with source-load coupling, (b) Resonator 1 and resonator 2 are fed without source-load coupling, (c) T_{z1} and T_{z2} are generated by source-load coupling, (d) Resonator 3 is fed with source-load coupling, (e) Resonator 3 is fed without source-load coupling, (f) T_{z3} and T_{z4} are generated by source-load coupling

Furthermore, from Fig. 7, it can be found that the four transmission zeros will move close to their passbands when the coupling length of source to load (expressed by S, as depicted in Fig. 1) is increased, thus, sharper attenuation shirts of the passbands can be achieved.

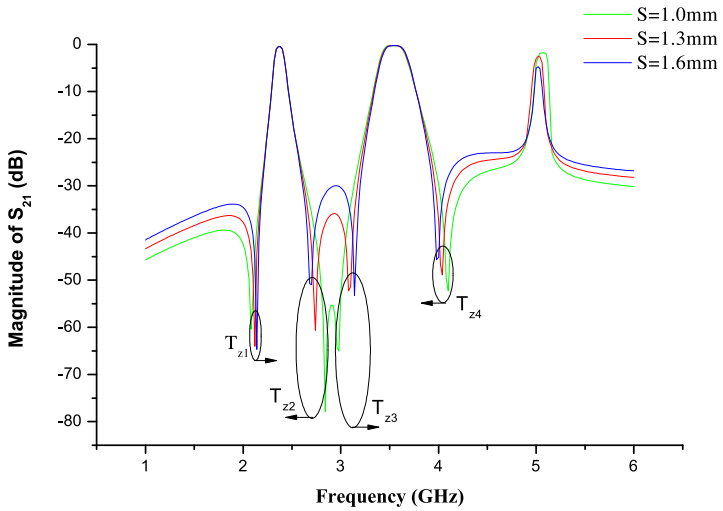

Fig. 7. Position of transmission zeros with varied S

Additionally, comparisons between the proposed tri-band filter and the referenced filters are listed in Table II. It can be found that the proposed filter has better performance on insertion loss and return loss, also, the size of the filter is compact.

© IEICE 2016
DOI: 10.1587/elex.13.20160605
Received June 20, 2016
Accepted June 27, 2016
Publicized July 11, 2016
Copyedited September 25, 2016

Table II. Comparisons between the proposed filter and other reported filters

Ref.	$1^{st}/2^{nd}/3^{rd}$ Passbands (GHz)	$\|S_{11}\|$ (dB)	$\|S_{21}\|$ (dB)	ε_r	Size ($\lambda_g \times \lambda_g$)
[1]	1.8/3.5/5.2	5/24/14	1.2/1.8/2	2.2	1.89×0.03
[2]	3/4.2/4.55	12/10/10	2.9/2.4/3.0	3.38	0.47×0.32
[3]	1.575/2.4/3.5	9/18.9/13.5	1.6/1.5/2.3	2.2	0.72×0.82
[4]	2.45/3.5/5.25	18/16/13	2/2.4/1.7	2.55	1.24×0.38
[5]	1.57/2.45/3.5	31/29/28	0.77/1.51/1.8	10.2	3.01×1.64
[6]	2.45/3.5/5.25	>13	0.9/1.7/2.1	2.65	0.93×1.14
[7]	2.4/3.5/5.2	>15	1.57/1.60/1.77	2.65	0.33×0.31
This Work	**2.4/3.5/5.15**	**25.6/34.2/16**	**0.89/0.74/1.7**	**3.48**	$\mathbf{0.41 \times 0.14}$

λ_g: the guided wavelength at the center frequency of the first passband

4 Conclusion

A novel planar tri-band BPF has been presented and analyzed in this letter. T-stub loaded stepped-impedance resonator (SIR) and short-circuited stub loaded uniform impedance resonator (UIR) are utilized to construct the proposed filter. Even-odd mode theory is introduced to study and explain its resonant characteristics. The measured results of the fabricated filter represent low passband insertion loss and good return loss. Source-load coupling is realized to improve the passband selectivity of the filter. The good performance, planar structure and compact size make it attractive for wireless communications.

Acknowledgments

The work is supported by National Natural Science Foundation of China (61563015) and Young Foundation of Humanities and Social Sciences of Ministry of Education in China (13YJCZH089).

© IEICE 2016
DOI: 10.1587/elex.13.20160605
Received June 20, 2016
Accepted June 27, 2016
Publicized July 11, 2016
Copyedited September 25, 2016